Received: 2 February 2017 | Revised: 29 April 2017 | Accepted: 1 May 2017

DOI: 10.1002/aoc.3899

FULL PAPER

WILEY Applied Organometallic Chemistry

Antimicrobial and anticancer activities of Schiff base ligand and its transition metal mixed ligand complexes with heterocyclic base

H. F. Abd El-Halim[1] | Gehad G. Mohamed[2] | Mahmoud N. Anwar[3]

[1] Pharmaceutical Chemistry Department, Faculty of Pharmacy, Misr International University, Cairo, Egypt

[2] Chemistry Department, Faculty of Science, Cairo University, Giza, Egypt

[3] Chemist, El-Nasr Co. for Intermediate Chemicals (NCIC), Giza, Egypt

Correspondence
H. F. Abd El-Halim, Pharmaceutical Chemistry Department, Faculty of Pharmacy, Misr International University, Cairo, Egypt.
Email: hanan.farouk2@yahoo.com

A new Schiff base ligand (HL) was prepared via a condensation reaction of quinoline-2-carboxaldhyde with 2-aminophenol in a molar ratio of 1:1. Its transition metal mixed ligand complexes with 1,10-phenanthroline (1,10-phen) as co-ligand were also synthesized in a 1:1:1 ratio. HL and its mixed ligand complexes were characterized using elemental analysis, infrared, ^{1}H NMR, mass and UV–visible spectroscopies, molar conductance, magnetic measurements, solid reflectance, thermal analysis, electron spin resonance and X-ray diffraction. Molar conductance measurements showed that all complexes have an electrolytic nature, except Cd(II) complex. From elemental and spectral data, the formulae $[M(L)(1,10\text{-phen})(H_2O)]Cl_x{\cdot}nH_2O$ (where M = Cr(III) ($x = n = 2$), Mn(II) and Ni(II) ($x = 1$, $n = 2$), Fe(III) ($x = n = 2$), Co(II), Cu(II) and Zn(II) ($x = 1$, $n = 2$)) and $[Cd(L)(1,10\text{-phen})Cl]{\cdot}3H_2O$ for the metal complexes have been proposed. The geometric structures of complexes were found to be octahedral. Powder X-ray diffraction reflected the crystalline nature of the complexes; however, the Schiff base is amorphous. HL and its mixed ligand complexes were screened against Gram-positive bacteria (*Streptococcus pneumoniae* and *Bacillus subtilis*) and Gram-negative bacteria (*Pseudomonas aeruginosa* and *Escherichia coli*). Antifungal activity was determined against *Aspergillus fumigatus* and *Candida albicans*, the data showing that most complexes had activity less than that of the Schiff base while Mn(II), Fe(III) and Ni(II) complexes showed no significant antifungal activity. The anticancer activity of HL and its metal complexes was also studied against breast and colon cell lines. The metal complexes showed IC_{50} higher than that of HL, especially the Cu(II) complex which showed the highest IC_{50} against breast cell line.

KEYWORDS

1,10-phen, anticancer activity, antimicrobial activity, mixed ligand complexes, thermal studies

1 | INTRODUCTION

Schiff bases as versatile organic blockers have recently attracted great attention due to their preparative accessibilities, structural varieties and varied denticities. Schiff base complexes have suitable biomimetic properties that can mimic the structural features of active sites, and they have been widely used in various fields such as biochemical reactions and biological regulation.[1,2] Quinoline is often used for the design of many synthetic Schiff bases with diverse pharmacological properties, such as antioxidant,[3] anti-inflammatory,[4] antimicrobial,[5] cytotoxic,[6] antiplasmodial[7] and anti-tumour[8] activities. In chemistry, Schiff bases of transition metal complexes have many applications as catalysts[9,10] and corrosion inhibitors.[11]

Recently, there have been many studies of mixed ligand complexes with nitrogen-containing heterocyclic amines

and Schiff base ligands. Chelating nitrogen donor ligands are among the most efficient chelators for transition metal and post-transition metal ions with which they form stable complexes in solution, and the presence of aromatic and/or heteroaromatic groups in the structure of nitrogen donors such as 1,10-phenanthroline (1,10-phen) gives these ligands additional properties and therapeutic, pharmacologic and DNA cleavage activity.[12–15]

In the work presented here, a new Schiff base (HL) derived from the condensation of quinoline-2-carboxaldhyde with 2-aminophenol was synthesized and mixed ligand complexes of Cr(III), Mn(II), Fe(III), Co(II), Ni(II), Cu(II), Zn(II) and Cd(II) were synthesized from HL with 1,10-phen as second ligand. The Schiff base ligand and its mixed ligand complexes were characterized using elemental and spectroscopic analyses. Antibacterial and antifungal activities of HL, 1,10-phen and the mixed ligand complexes were studied. The anticancer activity of HL and its mixed ligand complexes was also studied against two cell lines: breast cancer cell line (HCT-116) and colon cancer cell line (MCF-7).

2 | EXPERIMENTAL

2.1 | Materials

All chemicals were purchased and used without any purification. Quinoline-2-carboxaldehyde (Acros Organics, USA), 2-aminophenol (Cambrian Chemical), 1,10-phen (Merck, Germany) and metal chloride solids $CrCl_3{\cdot}6H_2O$, $MnCl_2{\cdot}2H_2O$ (Sigma), $FeCl_3{\cdot}6H_2O$ (Prolabo), $CoCl_2{\cdot}6H_2O$, $NiCl_2{\cdot}6H_2O$, $CuCl_2{\cdot}2H_2O$, $ZnCl_2{\cdot}2H_2O$ and $CdCl_2$ (BDH) were also used. Ethanol (99%, 95%) and dimethylformamide (DMF; 97%, Adwic) were used as organic solvents.

2.2 | Measurements

Microanalysis of carbon, hydrogen and nitrogen was carried out at the Microanalytical Center, Cairo University, Egypt, using a CHNS-932 (LECO) Vario elemental analyser. Metal ions were determined by titration against standard EDTA solution.[16–18] Fourier transform infrared (FT-IR) spectra was recorded with a PerkinElmer 1650 spectrometer (400–4000 cm^{-1}) using KBr pellets. ^1H NMR spectra, with samples as solutions in deuterated dimethylsulfoxide (DMSO-d_6), were recorded with a Varian Oxford Mercury 300 MHz NMR 300 at room temperature using tetramethylsilane as an internal standard. Mass spectra were obtained using the electron impact technique at 70 eV with an MS-5988 GS-MS Hewlett-Packard instrument at the Microanalytical Center, National Center for Research, Egypt. Molar conductivities of 10^{-3} M solutions of the solid complexes in DMF were measured using a Jenway 4010 conductivity meter. Melting points were measured with an SMP 30 (Stuart, UK). The molar magnetic susceptibility was measured using powdered samples with the Faraday method. The diamagnetic corrections were made by Pascal's constant and $Hg[Co(SCN)_4]$ was used as a calibrant. UV–visible spectra were obtained with UVmini-1240 UV–visible spectrophotometer (Shimadzu). Thermogravimetric (TG) analysis of the solid complexes was carried out using a Shimadzu TGA-50H thermal analyser, at a heating rate of 10°C min^{-1} from 25 to 1000°C in nitrogen atmosphere with a flow rate of 20 ml min^{-1}. Powder X-ray diffraction (XRD) analyses were carried out using a Philips Analytical BV type PW 1840 X-ray diffractometer. Radiation was provided by a copper target anode (2000 W) high-intensity X-ray tube operated at 40 kV and 30 mA. Divergence and receiving slits were 1° and 0.15 mm, respectively. Electron spin resonance (ESR) spectra were recorded with a JES-FE2XG ESR spectrophotometer at Atomic Energy Commission. Antibacterial, antifungal and anticancer activities were determined at the Regional Center for Mycology and Biotechnology, Al-Azhar University, Egypt.

2.3 | Syntheses

2.3.1 | Synthesis of Schiff base ligand

An ethanolic solution of 2-aminophenol (1.59 g, 3.18 mmol) was added to quinoline-2-carboxaldehyde (2.5 g, 3.18 mmol) dissolved in 50 ml of DMF in a 1:1 molar ratio. The mixture was refluxed for 2 h. A dark brown precipitate was developed, which was washed with a small amount of ethanol, then filtered, dried and weighed. The yield was 79%. The synthesis of the Schiff base ligand is presented in Scheme 1.

2.3.2 | Synthesis of mixed ligand complexes

An ethanolic solution of metal chloride salt (1.2 mmol) of Cr(III) (0.321 g), Mn(II) (0.195 g), Fe(III) (0.326 g), Co(II) (0.286 g), Ni(II) (0.285 g), Cu(II) (0.204 g), Zn(II) (0.206 g) and Cd(II) (0.217 g) was added to a mixture of 0.3 g (1.2 mmol) of Schiff base ligand dissolved in 50 ml of DMF and 0.22 g (1.2 mmol) of 1,10-phen dissolved in 20 ml of ethanol with a molar ratio of 1:1:1. The final mixture was refluxed for 2 h. Then the precipitates were washed with ethanol, filtered, dried and weighed. The synthesis of the mixed ligand complexes is presented in Scheme 2. The analytical and physical data of the complexes are summarized in Table 1.

2.4 | Antibacterial and antifungal activities

Antimicrobial activity was investigated using the agar well diffusion method.[19] The free Schiff base ligand (HL), 1,10-phen and the metal complexes of the mixed ligands were tested *in vitro* for their antibacterial activity against

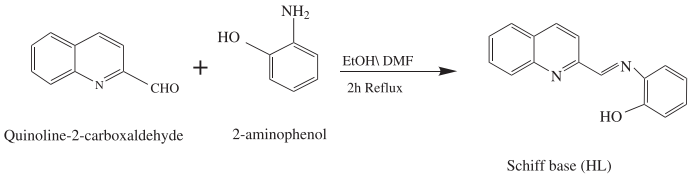

SCHEME 1 Synthesis of the Schiff base ligand (HL)

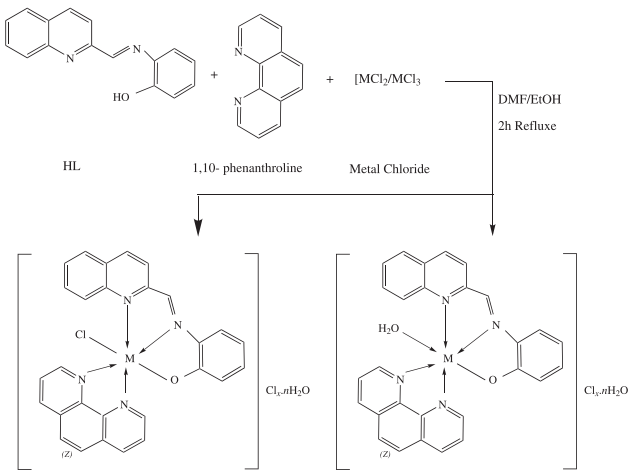

SCHEME 2 Synthesis of mixed ligand complexes of (HL) with (1,10-phen), (a) M = Cr(III) and Fe (III) (x = n = 2), Mn(II) and Ni(II) (x = 1, n = 3), Co(II), Cu(II) and Zn(II) (x = 1, n = 2); (b) Cd(II) complex

Gram-positive bacteria (*Streptococcus pneumoniae* (RCMB010010) and *Bacillus subtilis* (RCMB 010067)) and Gram-negative bacteria (*Pseudomonas aeruginosa* (RCMB 010043) and *Escherichia coli* (RCMB 010052)). Antifungal activity was investigated against *Aspergillus fumigatus* (RCMB 02568) and *Candida albicans* (RCMB 05036) using Sabourauad Dextrose Agar medium. Gentamicin, ampicillin and amphotericin B were used as standard drugs for Gram-positive bacterial, Gram-negative bacterial and antifungal activity, respectively. DMSO was used as solvent control. The compounds were tested at a concentration of 5 mg ml^{-1} against bacterial and fungal strains. Sterilized media were poured onto sterilized Petri dishes (20 ml each dish) and allowed to solidify. Wells of 6 mm in diameter were made in the solidified media with the help of sterile borer. A sterile swab was used to evenly distribute microbial suspension over the surface of solidified media and solution and the test samples were added to each well using a micropipette. The plates were incubated at 37°C for 24 h in the case of antibacterial activity and at 25°C for 48 h for antifungal activity. These tests were carried out in triplicate and zones of inhibition were measured in millimetres.

2.5 | Anticancer Activity

Cytotoxicity evaluation was carried out using viability assay. The free Schiff base ligand, 1,10-phen and the mixed ligand

TABLE 1 Analytical and physical data for Schiff base ligand (HL) and its complexes with 1,10-phen

Compound	Colour Yield (%)	M.p. (°C)	Conductivity (S mol^{-1} cm^2)	μ_{eff} (BM)	Elemental analysis (%): Found (calcd)			
					C	H	N	M
HL	Brown 79	197	—	—	77.53 (77.42)	4.54 (4.84)	11.70 (11.29)	—
[Cr(L)(1,10-phen)(H_2O)]Cl_2.2H_2O	Brown 87.24	320	146.1	4.47	55.59 (55.62)	4.10 (4.13)	9.20 (9.27)	8.62 (8.60)
[Mn(L)(1,10-phen)(H_2O)]Cl.3H_2O	Brown 88.9	335	71.30	5.35	56.95 (57.09)	4.34 (4.59)	9.50 (9.52)	9.60 (9.18)
[Fe(L)(1,10-phen.)(H_2O)]Cl_2.2H_2O	Black 83.7	233	179.0	5.37	55.24 (55.26)	4.82 (4.44)	9.23 (9.21)	9.16 (9.21)
[Co(L)(1,10-phen)(H_2O)]Cl.2H_2O	Black 95.5	142	97.50	5.43	57.66 (57.38)	4.52 (4.27)	9.34 (9.56)	10.21 (10.15)
[Ni(L)(1,10-phen)(H_2O)]Cl.3H_2O	Black 83.9	260	71.70	3.13	56.94 (56.42)	4.34 (4.53)	9.03 (9.40)	10.10 (10.24)
[Cu(L)(1,10-phen)(H_2O)]Cl.2H_2O	Black 96.25	250	83.20	1.82	57.62 (57.97)	4.09 (4.31)	9.19 (9.66)	10.24 (10.87)
[Zn(L)(1,10-phen)(H_2O)]Cl.2H_2O	Brown 98.9	273	57.50	Diamagnetic	57.60 (57.78)	4.42 (4.30)	9.61 (9.63)	11.52 (11.18)
[Cd(L)(1,10-phen)Cl].3H_2O	Brown 83.9	>350	25.70	Diamagnetic	53.01 (53.46)	4.14 (3.98)	8.72 (8.91)	17.42 (17.82)

complexes were tested against breast cell line (MCF-7) and colon cell line (HCT-116). The cells were propagated in Dulbecco's modified Eagle's medium supplemented with 10% heat-inactivated foetal bovine serum, 1% L-glutamine, HEPES buffer and 50 μg ml^{-1} gentamycin. All cells were maintained at 37°C in a humidified atmosphere with 5% CO_2 and were sub-cultured two times a week. For cytotoxicity assay, the cells were seeded in a 96-well plate at a cell concentration of 1×10^4 cells per well in 100 μl of growth medium. Fresh medium containing different concentration of the test sample was added after 24 h of seeding. Serial twofold dilutions of the test chemical compound were added to confluent cell monolayers in 96-well, flat-bottomed microtitre plates (Falcon, NJ, USA) using a multichannel pipette. The microtitre plates were incubated at 37°C in a humidified incubator with 5% CO_2 for a period of 48 h. Three wells were used for each concentration of test sample. Control cells were incubated without test sample and without DMSO. The small percentage of DMSO present in the wells (maximal 0.1%) was found not to affect the experiment. After incubation of wells for 24 h at 37°C, various concentrations of sample (50, 25, 12.5, 6.25, 3.125 and 1.56 μg) were added, and the incubation was continued for 48 h and viable cell yield was determined using a colorimetric method. The 50% inhibitory concentration (IC_{50}), the concentration required to cause toxic effects in 50% of cells, was estimated from graphic plots. In brief, after the end of the incubation period, media were aspirated and crystal violet solution (1%) was added to each well for at least 30 min. The stain was removed and the plates were rinsed using tap water until all excess stain was removed. Glacial acetic acid (30%) was then added to all wells and mixed thoroughly, and then the absorbance of the plates was measured after being gently shaken using a microplate reader (TECAN Inc.), with a test wavelength of 490 nm. All results were corrected for background absorbance measured in wells without added stain. Treated samples were compared with the cell control in the absence of the test compounds. All experiments were carried out in triplicate. The cell cytotoxic effect of each tested compound was calculated.[20]

3 | RESULTS AND DISCUSSION

3.1 | Elemental analyses

The results of elemental analyses with suggested molecular formula and physical properties of the Schiff base ligand and mixed ligand complexes are listed in Table 1. The Schiff base ligand and its mixed ligand complexes are insoluble in most organic solvents, except DMF and DMSO.

3.2 | Molar conductivity measurements

The molar conductance values of the synthesized complexes in DMF as a solvent with a concentration of 1×10^{-3} M at room temperature are listed in Table 1. The Cd(II) complex showed a non-electrolytic nature. However, the molar conductance values of Mn(II), Co(II), Ni(II), Cu(II) and Zn(II) complexes indicated that these chelates were ionic in nature and they were type 1:1 electrolytes. Cr(III) and Fe(III) complexes were 1:2 electrolytes.

3.3 | Magnetic susceptibility and electronic spectral studies

The magnetic moments of the Schiff base mixed ligand complexes were recorded at room temperature (25°C). The calculated values are listed in Table 1. The μ_{eff} values of Cr(III), Mn(II), Fe(III), Co(II), Ni(II) and Cu(II) complexes indicated octahedral geometry around the metal ions. As Zn(II) and Cd(II) complexes were diamagnetic, an octahedral geometry was also proposed for these complexes referring to their elemental analysis and spectroscopic analytical data and their empirical formula.[12,21]

Absorption spectral of HL and its mixed ligand complexes were obtained in DMF. UV–visible spectra were recorded for 1×10^{-4} M prepared solutions in the range 200–700 nm. A band at 267 nm was observed which may be attributed to π–π* transition of the aromatic ring. A second band observed at 310 nm could be attributed to n– π* electronic transition of azomethine group in HL.[14,22] Both bands were highly shifted (bathochromic shift) in the spectra of mixed ligand complexes to 269–296 and 320–350 nm, respectively, due to chelation with metal ions. The spectra of Cr(III), Mn(II), Fe(III), Co(II), Ni(II), Cu(II), Ni(II), Zn(II) and Cd(II) complexes also showed absorption bands at 430, 450, 440, 455, 435, 425, 420 and 425 nm which may be assigned to the splitting of d–d orbital. For Co(II), Ni(II) and Cu(II) complexes a band at 332 nm appeared which may be attributed to ligand-to-metal charge transfer.[21]

3.4 | Diffuse reflectance spectra

The diffuse reflectance spectrum of the Cr(III) complex showed three bands at 28 089, 25 773 and 19 342 cm^{-1}, respectively, which may be assigned to $^4A_{2g} \rightarrow {}^4T_{2g}(F)$, $^4A_{2g} \rightarrow {}^4T_{1g}(F)$ and $^4A_{2g}(F) \rightarrow {}^4T_{1g}(P)$ transitions.[12,22] The diffuse reflectance spectrum of the Mn(II) complex showed three bands at 26 351, 18 726 and 15 873 cm^{-1}, respectively, which may correspond to $^4T_{1g} \rightarrow {}^6A_{1g}$, $^4T_{2g}(G) \rightarrow {}^6A_{1g}$ and $^4T_{1g}(D) \rightarrow {}^6A_{1g}$ transitions.[12,22,23] The diffused reflectance spectrum of the Fe(III) complex showed two bands at 22 988 and 17 699 cm^{-1} which may be assigned to $^6A_{1g} \rightarrow T_{2g}(G)$ and $^6A_1 \rightarrow {}^5T_{1g}$ transitions. The spectrum also showed a band at 24 752 cm^{-1} which may be attributed to ligand-to-metal charge transfer.[23] The diffuse reflectance spectrum of the Co(II) complex showed three bands at 21 978, 17 421 and 15 797 cm^{-1}, respectively,

assigned to $^4T_{1g} \rightarrow {}^4T_{2g}(F)$, $^4T_{1g} \rightarrow {}^4A_{2g}(F)$ and $^4T_{1g}(F) \rightarrow {}^4T_{1g}(P)$ transitions.[12,22] The spectrum showed also a band at 28 571 cm^{-1} which may be attributed to ligand-to-metal charge transfer. The spectrum of the Ni(II) complex showed three bands at 20 000, 17 421 and 15 873 cm^{-1}, respectively, which may correspond to $^3A_{2g}(F) \rightarrow {}^3T_{1g}(P)$, $^3A_{2g}(F) \rightarrow {}^3T_{1g}(F)$ and $^3A_{2g}(F) \rightarrow {}^3T_{1g}$ transitions. The spectrum also showed a band at 28 169 cm^{-1} that may be attributed to ligand-to-metal charge transfer.[12,22] The spectrum of the Cu(II) complex showed two bands at 15 873 and 20 491 cm^{-1} respectively, corresponding to $^2E_g \rightarrow {}^2T_{2g}(D)$ and $^2B_{1g} \rightarrow {}^2A_{1g}$ transitions. The spectrum also showed a band at 24 630 cm^{-1} which may be attributed to ligand-to-metal charge transfer.

3.5 | FT-IR spectra

The FT-IR spectral data for HL and its mixed ligand complexes are listed in Table 2. The FT-IR spectrum of HL showed a band at 1662 cm^{-1} assigned to azomethine group ν(CH═N).[15,24] A broad band at 3440 cm^{-1} appeared due to the phenolic group ν(─OH) which disappeared during complexation.[15,24] A medium intensity band appeared at 1282 cm^{-1} which was assigned to phenolic group ν(C─O) in the complexes.[15] Formation of mixed ligand complexes was confirmed by significant shifts in the bands of stretching vibrations ν(CH═N), ν(C─O) and ν(─OH). The band of azomethine ν(CH═N) was shifted by 11–27 cm^{-1} to lower frequency in the spectra of the complexes indicating its involvement in coordination. The ν(C─O) band was also shifted to higher frequencies by 18–37 cm^{-1} indicating chelation through deprotonated phenolic group.[24] The broad absorption band in the region 3410–3440 cm^{-1} was assigned to the ν(─OH) vibration of hydrated or coordinated water molecules accompanied by characteristic bending band in the region 835–852 cm^{-1}.[12,21,24] A band at 1126 cm^{-1} assigned to benzene and pyridine ring stretching vibration in free 1,10-phen was decreased by 15–27 cm^{-1} indicating coordination via nitrogen atoms.[12] The FT-IR spectrum of the free Schiff base ligand showed a sharp and strong band at 1592 cm^{-1}, which could be attributed to the ν(C═N) vibration of the pyridyl ring.[10] The band was shifted to higher frequencies (22–32 cm^{-1}) indicating the involvement of the nitrogen atom of pyridine in the coordination sphere. New bands appeared in the regions 424–474 and 524–578 cm^{-1} for M─N and M─O, respectively, indicating the complexation of metal ions via N and O atoms of the ligand.[12,21]

3.6 | ^{1}H NMR spectra

The ^{1}H NMR spectrum of HL was characterized by singlet proton of azomethine group (CH═N) appearing at 8.65 ppm (s, 1H). Multiple signals at 6.38–8.13 ppm (m, 10H) corresponding to the aromatic ring and quinoline also appeared. A characteristic singlet signal of OH proton at 10.8 ppm (s, 1H) appeared. The ^{1}H NMR spectra of Zn(II) and Cd(II) complexes were characterized by significant downfield shifts in the signal position of azomethine (CH═N) proton to 9.07, 8.92 ppm (s, 1H) which indicated complexation via azomethine group. Also, the resonance of aromatic protons was shifted downfield to 6.48–8.56 and 6.47–8.7 ppm (m, 18H), respectively, as a result of coordination of nitrogen atoms of quinoline and 1,10-phen to metal ions.[25] Signals at 3.33 ppm (s, 4H) and 3.287 ppm (s, 6H) appeared due to the presence of hydrated water in Zn(II) and Cd(II) complexes, respectively.[12]

3.7 | Mass spectra

The electron impact mass spectra of HL and its Cr(III) complex were recorded and investigated at an electron energy of 70 eV. The mass spectra of HL and Cr(III) complex were

TABLE 2 Characteristic FT-IR bands (cm^{-1}) for Schiff base ligand (HL) and its complexes with 1,10-phen[a]

Compound	ν(H_2O)	ν(OH)	ν(CH═N)	ν(─C─O)	Stretching benzene, pyridine ring	ν(C═N) pyridyl ring of quinoline	ν(M─N)	ν(M─O)
HL	—	3440 b	1662 s	1282 m	—	1592 w	—	—
1,10-phen	—	—	—	—	1126 w	—	—	—
[Cr(L)(1,10-phen)(H_2O)]Cl_2.2H_2O	3435b	—	1635 w	1319 w	1107 w	1562 w	439 w	524 w
[Mn(L)(1,10-phen)(H_2O)]Cl.3H_2O	3410 b	—	1647 w	1300 m	1099 m	1560 w	474 w	551 w
[Fe(L)(1,10-phen)(H_2O)]Cl_2.2H_2O	3430 b	—	1640 w	1315 m	1111 m	1565 w	466 w	555 w
[Co(L)(1,10-phen)(H_2O)]Cl.2H_2O	3440 b	—	1651 w	1307 m	1107 m	1562 w	424 w	524 w
[Ni(L)(1,10-phen)(H_2O)]Cl.3H_2O	3425 b	—	1640 w	1300 m	1103 w	1560 w	459 w	528 w
[Cu(L)(1,10-phen)(H_2O)]Cl.2H_2O	3421 b	—	1637 w	1315 m	1099 w	1570 w	439 w	540 w
[Zn(L)(1,10-phen)(H_2O)]Cl.2H_2O	3430 b	—	1644 w	1300 m	1103 w	1566 w	470 w	578 w
[Cd(L)(1,10-phen)Cl].3H_2O	3420 b	—	11640 w	1300 w	1103 s	1560 w	424 w	524 w

[a]w: weak; b: broad; m: medium; s: sharp.

characterized by moderate to high relative intensity molecular ion peaks. The abundance of the molecular ion depends mainly on the structure. The molecular ion peak of the ligand was found at $m/z = 248$ amu and at $m/z = 604$ amu for the Cr(III) complex. The peaks of fragmentation were confirmed with suggested fragments shown in Scheme 3(a) for HL and in Scheme 3(b) for the Cr(III) complex.

3.8 | Thermal analyses

TG analysis results of HL and its mixed ligand complexes are summarized in Table 3. The Schiff base ligand decomposed in two steps within the range from 150 to 700°C with total mass loss of 100% (calcd 100%). The first step occurred within the range 150–465°C involving a mass loss of 37.50% (calcd 37.90%) corresponding to loss of C_6H_6O molecule. The second step occurred within the range 365–700°C with mass loss of 62.50% (calcd 62.09%) corresponding to the loss of $C_{10}H_6N_2$ molecule.

The TG curve of $[Cr(L)(1,10\text{-phen})(H_2O)]Cl_2{\cdot}2H_2O$ complex showed three decomposition steps within the range 40–800°C with total mass loss of 83.47% (calcd 83.44%). The first step occurred within the range 40–170°C with mass loss of 4.46% (calcd 4.47%) corresponding to loss of hydrated water molecules. The second step occurred within the range 170–410°C with mass loss of 25.16% (calcd 25.00%) corresponding to loss of two HCl and C_5H_4N molecule. The third step occurred within the range 410–770°C with mass loss of 53.85% (calcd 53.97%) corresponding to loss of $C_{21}H_{16}N_3O$ molecule. Finally, 16.56% (calcd 16.55%) metallic residue remained in a form of metal oxide ($½(Cr_2O_3)$) contaminated with carbon.

$[Mn(L)(1,10\text{-phen})(H_2O)]Cl{\cdot}3H_2O$ complex showed three decomposition steps within the range 50–800°C with total mass loss of 83.68% (calcd 84.25%). The first step occurred within the range 50–165°C in two stages with mass loss of 9.17% (calcd 9.18%) corresponding to loss of three hydrated water and coordinated water molecules. The second step occurred within the range 165–600°C in two stages with mass loss of 45.28% (calcd 45.34%) corresponding to loss of HCl and $C_{16}H_{10}N_2$ molecules. The third step occurred within the range 600–800 °C with mass loss of 29.23% (calcd 29.73%) corresponding to loss of $C_{10}H_8N_2O$ molecule. Finally, 16.32% (calcd 15.75%) metallic residue remained in a form of metal oxide (MnO) contaminated with carbon.

$[Fe(L)(1,10\text{-phen.})(H_2O)]Cl_2{\cdot}2H_2O$ complex showed three decomposition steps within the range 40–800°C with total mass loss of 81.57% (calcd 81.58%). The first step occurred within the range 40–375°C in three stages with mass loss of 23.10% (calcd 23.11%) corresponding to loss of hydrated water molecules and C_6H_6Cl molecule. The second step occurred within the range 375–500°C in two stages with mass loss of 29.52% (calcd 29.52%) corresponding to loss of $C_9H_8N_2Cl$ molecule. The third step occurred within the range 500–800 °C with mass loss of 28.94% (calcd 28.95%) corresponding to loss of $C_{10}H_{12}N_2O$ molecule. Finally, 18.43% (calcd 18.10%) metallic residue remained in a form of metal oxide ($½(Fe_2O_3)$) contaminated with carbon.

$[Co(L)(1,10\text{-phen})(H_2O)]Cl{\cdot}2H_2O$ complex showed four decomposition steps within the range 40–800°C with total mass loss of 85.85% (calcd 86.50%). The first step occurred within the range 40–200°C in two stages with mass loss of 9.22% (calcd 9.28%) corresponding to loss of two hydrated and coordinated water molecules. The second step occurred within the range 200–400°C in two stages with mass loss of 20.10% (calcd 20.12%) corresponding to loss of C_5H_8NCl molecule. The third step occurred within the range 400–525°C with mass loss of 21.68% (calcd 22.00%) corresponding to loss of $C_8H_4N_2$ molecule. The fourth step occurred within the range 525–800°C with mass loss of 34.67% (calcd 35.00%) corresponding to loss of $C_{15}H_9N$ molecule. Finally, 14.15% (calcd 13.50%) metallic residue remained in a form of metal oxide CoO.

$[Ni(L)(1,10\text{-phen})(H_2O)]Cl{\cdot}3H_2O$ complex showed two decomposition steps within the range 25–700°C with total mass loss of 82.83% (calcd 83.03%). The first step occurred within the range 25–440°C in two stages with mass loss of

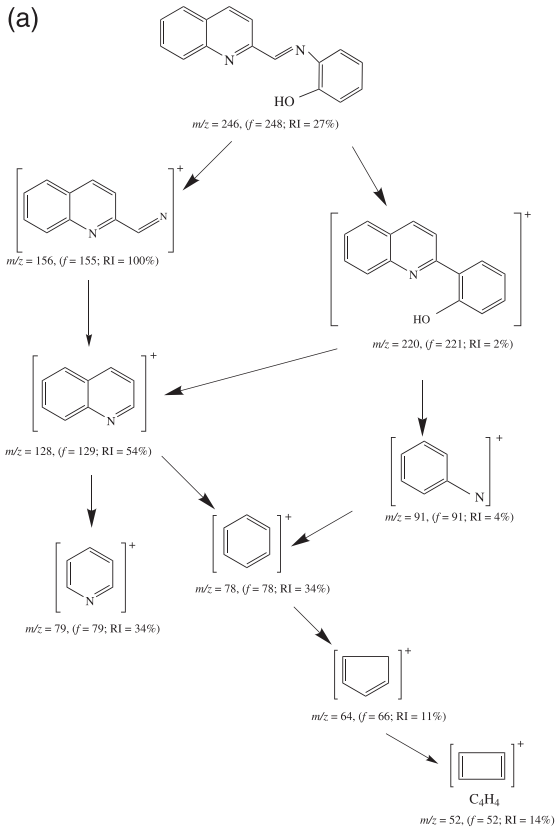

SCHEME 3 (a) Mass fragmentation pattern of Schiff base ligand HL

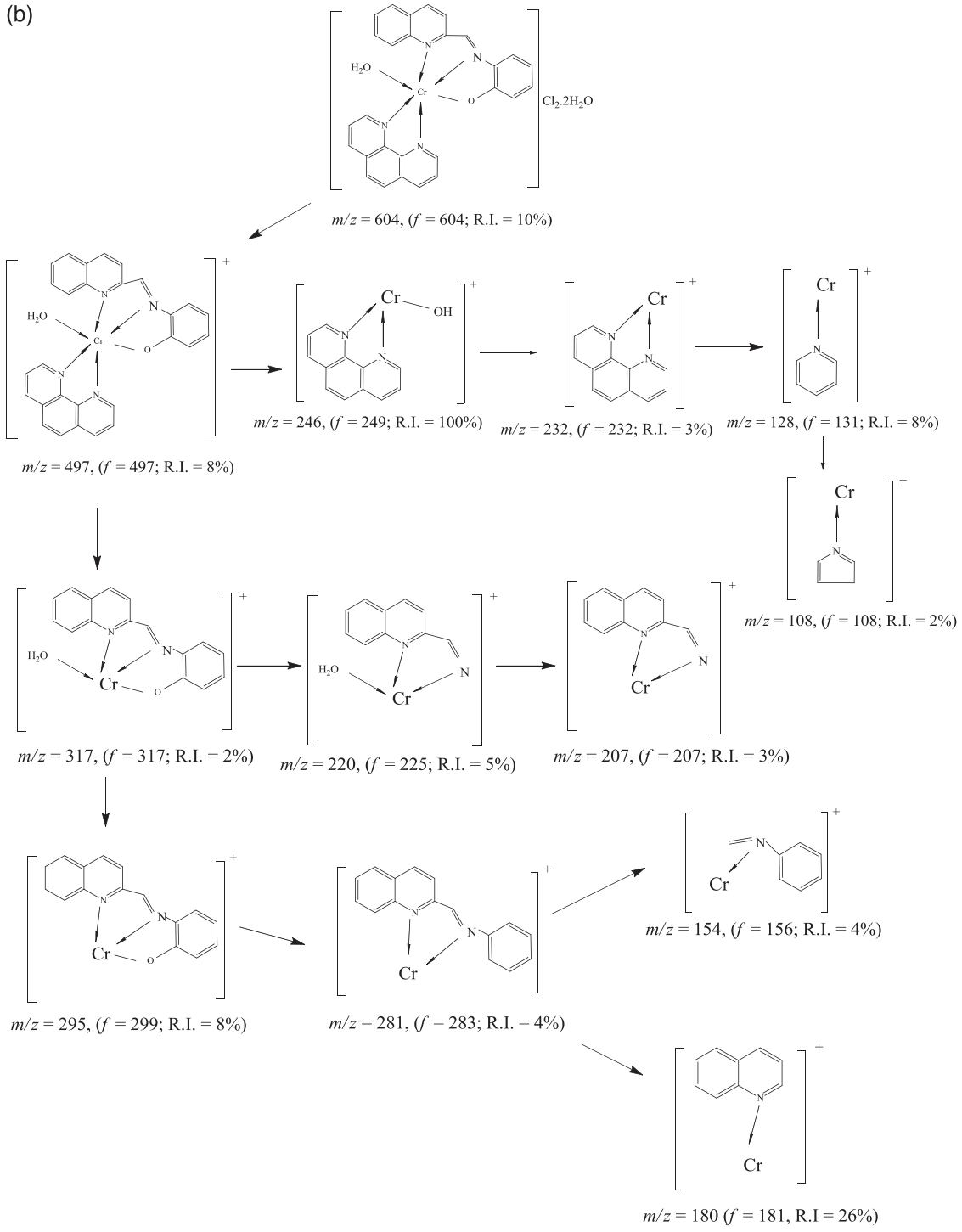

SCHEME 3 (b) Mass pattern of $[Cr(L)(1,10\text{-phen})H_2O]Cl_2.2H_2O$ complex

41.00% (calcd 41.22%) corresponding to loss of three water molecules of hydration and coordinated water molecule, then loss of organic moiety $C_{10}H_8N_2Cl$. The second step occurred within the range 440–700°C with mass loss of 41.83% (calcd 41.81%) corresponding to loss of $C_{14}H_{13}N_2$ molecule. Finally, 17.17% (calcd 16.97%) metallic residue remained in a form of metal oxide (NiO) contaminated with carbon.

$[Cu(L)(1,10\text{-phen})(H_2O)]Cl{\cdot}2H_2O$ complex showed two decomposition steps within the range 40–800°C with total mass loss of 81.80% (calcd 82.60%). The first step occurred within the range 40–470°C in two stages with mass loss of 46.00% (calcd 46.50%) corresponding to loss of two hydrated water and coordinated water molecules, then loss of organic moiety $C_{12}H_8N_2Cl$. The second step occurred within the range 470–770 °C with mass loss of 35.80%

TABLE 3 Thermal decomposition of Schiff base ligand and its metal complexes with 1,10-phen

Compound	Temp. range (°C)	n^a	DTA_{max} (°C)	Mass loss (%): calcd (found)	Total mass loss (%): calcd (found)	Assignment	Metallic residue
HL	150–465	1	285	38.71 (38.73)	100 (100)	Loss of C_6H_6O	—
	465–700	1	610	61.29 (61.27)		Loss of $C_{10}H_8N_2$	
[Cr(L)(1,10-phen)(H_2O)] $Cl_2.2H_2O$	40–170	1	90	4.47 (4.46)	83.44 (83.47)	Loss of $1_{1/2}H_2O$	½(Cr_2O_3) + 2C
	170–410	2	260, 350	25.00 (25.16)		Loss of C_5H_4N + 2HCl	
	410–800	1	540	53.97 (53.85)		Loss of $C_{21}H_{16}N_3O$	
[Mn(L)(1,10-phen)(H_2O)] $Cl.3H_2O$	50–165	2	85, 140	9.18 (9.17)	84.25 (83.68)	Loss of $3H_2O$	MnO + 2C
	165–600	2	240, 490	45.34 (45.28)		Loss of $C_{16}H_{10}N_2$ + HCl	
	600–800	1	680	29.73 (29.23)		Loss of $C_{10}H_8N_2O$	
[Fe(L)(1,10-phen)(H_2O)] $Cl_2.2H_2O$	40–475	3	80,200, 325	23.11 (23.10)	81.58 (81.57)	Loss of $1_{1/2}H_2O$ + C_6H_6Cl	½(Fe_2O_3) +3C
	375–500	2		29.52 (29.52)		Loss of $C_9H_8N_2Cl$	
	500–800	1	385, 430 600	28.95 (28.95)		Loss of $C_{10}H_{12}N_2O$	
[Co(L)(1,10-phen)(H_2O)] $Cl.2H_2O$	40–200	2	95, 150	9.28 (9.22)	86.50 (85.85)	Loss of $3H_2O$	CoO
	200–400	2	250, 310	20.12 (20.10)		Loss of C_5H_8NCl	
	400–525	1	490	22.00 (21.86)		Loss of $C_8H_4N_2$	
	525–800	1	640	35.10 (34.67)		Loss of $C_{15}H_9N$	
[Ni(L)(1,10-phen)(H_2O)] $Cl.3H_2O$	25–440	2	80, 300	41.22 (41.00)	83.03 (82.83)	Loss of $3H_2O$ + $C_{10}H_8N_2Cl$	NiO +2C
	440–700	1	620	41.81 (41.83)		Loss of $C_{16}H_{13}N_2O$	
[Cu(L)(1,10-phen)(H_2O)] $Cl.2H_2O$	40–470	2	80, 300	46.30 (56.00)	82.60 (81.80)	Loss of $3H_2O$ + $C_{12}H_8N_2Cl$	CuO + 2C
	470–770	1	640	36.10 (35.80)		Loss of $C_{14}H_7N_2$	
[Zn(L)(1,10-phen)(H2O)] $Cl.2H_2O$	45–425	2	80, 315	28.80 (28.80)	81.94 (81.93)	Loss of $3H_2O$ + C_6H_6Cl	ZnO + 2C
	425–525	1	480	26.83 (26.82)		Loss of $C_{10}H_8N_2$	
	525–750	1	720	26.31 (26.31)		Loss of $C_{10}H_5N_2$	
[Cd(L)(1,10-phen)Cl].$3H_2O$	45–425	2	80, 320	30.47 (30.46)	75.82 (75.79)	Loss of $3H_2O$ + C_8H_6Cl	CdO + 2C
	425–530	1	475	24.82 (24.81)		Loss of $C_{10}H_8N_2$	
	530–750	1	700	20.53 (20.52)		Loss of $C_8H_5N_2$	

[a]Number of decomposition stage.

(calcd 36.10%) corresponding to loss of $C_{14}H_7N_2O$ molecule. Finally, 18.27% (calcd17.40%) metallic residue remained in a form of metal oxide (CuO) contaminated with carbon.

[Zn(L)(1,10-phen)(H_2O)]Cl·$2H_2O$ complex showed three decomposition steps within the range 45–750°C with total mass loss of 81.93% (calcd 81.94%). The first step occurred within the range 45–425 °C in two steps with mass loss of 28.80% (calcd 28.80%) corresponding to loss of two hydrated water and coordinated water molecules, then loss of organic moiety C_6H_6Cl. The second step occurred within the range 425–525°C with mass loss of 26.82% (calcd 26.83%) corresponding to loss of $C_{10}H_8N_2$ molecule. The third step occurred within the range 525–750°C with mass loss of 26.31% (calcd 26.31%) corresponding to loss of $C_{10}H_5N_2$ molecule. Finally, 18.10% (calcd 18.10%) metallic residue remained in a form of metal oxide (ZnO) contaminated with carbon.

[Cd(L)(1,10-phen)Cl]·$3H_2O$ complex showed three decomposition steps within the range 45–750 °C with total mass loss of 75.79% (calcd 75.82%). The first step occurred within the range 75–425°C in two stages with mass loss of 30.46% (calcd 30.47%) corresponding to loss three water molecules of hydration and loss of organic moiety C_8H_6Cl. The second step occurred within the range 425–530 °C with mass loss of 24.81% (calcd 24.82%) corresponding to loss of $C_{10}H_8N_2$ molecule. The third step occurred within the range 530–750 °C with mass loss of 20.52% (calcd 20.53%) corresponding to loss of $C_8H_5N_2$ molecule. Finally, 24.21% (calcd 24.18%) metallic residue remained in a form of metal oxide (CdO) contaminated with carbon.

3.9 | ESR study

The solid-state ESR spectrum of the Cu(II) complex exhibited axially symmetric g-tensor parameters with $g_{\parallel} < g_{\perp}$ (2.059) > 2.0023 indicating that the copper site has a $d_{x^2-y^2}$ ground state characteristic of octahedral stereochemistry.[21,26] Kivelson and Neiman[27] reported a $g_{\parallel}$ value less than 2.3 for covalent character of a metal–ligand bond and greater than 2.3 for ionic character. In the Cu(II) complex, $g_{\parallel} = 2.08$ indicating a covalent character of the metal–ligand bond. The trend $g_{\parallel}$ (2.077) > $g_{\perp}$ (2.059) > g_e (2.0023)

observed for this complex indicated that the unpaired electron was localized in $d_{x^2-y^2}$ orbital of the Cu(II) ion and the spectral features were characteristic for axial symmetry.[28] In axial symmetry, the g-values are related by the expression $G = (g_{\parallel} - 2)/(g_{\perp} - 2) = 4$, where G is the exchange interaction parameter. According to Hathaway and Billing,[29] if the value of G is greater than 4, the exchange interaction between Cu(II) centres in the solid state is negligible, whereas when G is less than 4, considerable exchange interaction is indicated in the solid complex. The observed value for the exchange interaction parameter of $G = 1.3$ suggested that significant exchange coupling was present.

3.10 | Powder XRD study

The XRD patterns of mixed ligand complexes showed a crystalline nature; however, that of the Schiff base ligand showed an amorphous nature. This confirmed that the presence of metal ions changed the XRD pattern of the free Schiff base ligand.[30]

The average crystallite size (ξ) can be calculated from the XRD pattern according to the Debye–Scherrer equation:[31,32]

$$\xi = \frac{K\lambda}{\beta_{1/2}\cos\theta} \quad (1)$$

where λ is the wavelength of X-ray radiation (1.542475 Å), K is a constant taken as 0.95 for organic compounds and $\beta_{1/2}$ is the width at half maximum of the reference diffraction peak measured in radians.

The dislocation density (δ) indicates the number of dislocation lines per unit area of the crystal. The value of δ is related to the average particle diameter (ξ) through the relation[33,34]

$$\delta = \frac{1}{\xi^2} \quad (2)$$

The calculated values of ξ for Cr(III), Mn(II), Fe(III), Co(II), Ni(II), Cu(II), Zn(II) and Cd(II) complexes were found to be 41.73, 39.83, 29.03, 28.10, 35.88, 27.33, 28.72 and 40.68 nm, respectively. The value of δ for the complexes was found to be 0.00057, 0.00063, 0.00118, 0.00127, 0.00078, 0.00134, 0.00121 and 0.00061 nm^{-2}, respectively.

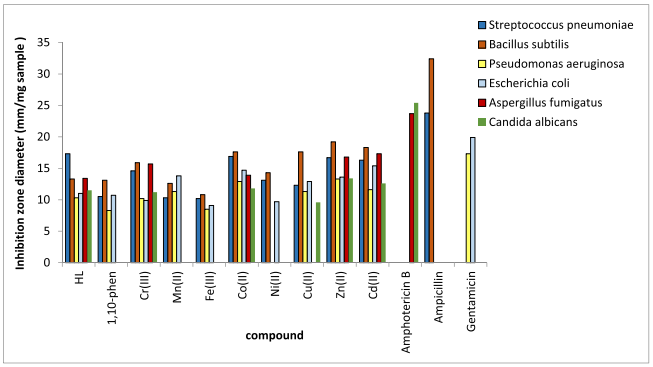

FIGURE 1 Antimicrobial (antibacterial, antifungal) activities of Schiff base ligand and its complexes

TABLE 4 Antimicrobial (antibacterial and antifungal) activities of Schiff base ligand (HL) and complexes with 1,10-phen

	Inhibition zone diameter (mm mg^{-1})					
	Antibacterial					
	Gram (+)		Gram (−)		Antifungal	
Compound	*S. pneumoniae*	*B. subtilis*	*P. aeruginosa*	*E. coil*	*A. fumigatus*	*C. albicans*
HL	17.3	13.3	10.3	10.9	13.4	11.5
1,10-phen	10.5	13.1	8.3	10.7	NA	NA
$[Cr(L)(1,10\text{-phen})(H_2O)]Cl_2.2H_2O$	14.6	15.9	10.2	9.8	15.7	11.2
$[Mn(L)(1,10\text{-phen})(H_2O)]Cl.3H_2O$	10.3	12.6	11.3	13.8	NA	NA
$[Fe(L)(1,10\text{-phen})(H_2O)]Cl_2.2H_2O$	10.2	10.8	8.5	9.1	NA	NA
$[Co(L)(1,10\text{-phen})(H_2O)]Cl.2H_2O$	16.9	17.6	12.9	14.7	13.9	11.8
$[Ni(L)(1,10\text{-phen})(H_2O)]Cl.3H_2O$	13.1	14.3	NA	9.7	NA	NA
$[Cu(L)(1,10\text{-phen})(H_2O)]Cl.2H_2O$	12.3	17.6	11.3	12.9	NA	9.7
$[Zn(L)(1,10\text{-phen})(H_2O)]Cl.2H_2O$	16.7	19.2	13.3	13.6	16.8	13.4
$[Cd(L)(1,10\text{-phen})Cl].3H_2O$	16.3	18.3	11.6	15.4	17.3	12.6
Amphotericin B	—	—	—	—	23.7	19.7
Ampicillin	23.8	32.4	—	—	—	—
Gentamicin	—	—	17.3	19.9	—	—

3.11 | Biological activity

3.11.1 | Antibacterial activity

The biological activity of metal complexes is affected by several factors, including the chelate effect of the ligands, the nature of the donor atoms/metal ions/counter ions that neutralize the complex, the total charge on the complex ion and the geometric structure of the complex.[35,36] Furthermore, chelation reduces the polarity of the metal ion because of partial sharing of its positive charge with the donor groups and possibly p-electron delocalization within the whole chelate ring system that is formed during coordination.[37] All these factors increase the lipophilicity of the central metal atom and hence increase the hydrophobic character and liposolubility of the complex favouring its permeation through the lipid layer of a bacterial membrane. This enhances the rate of uptake/entrance and thus the antibacterial activity of the test compounds.

The antibacterial activities of HL, 1,10-phen and mixed ligand complexes are summarized in Table 4 and shown in Figure 1. Screening against Gram-positive bacterium *S. pneumoniae* showed that the activity of all metal complexes was less than that of HL. The results for *B. subtilis* showed that the activities of Cr(III), Co(II), Ni(II), Cu(II), Zn(II) and Cd(II) complexes were higher than that of HL. However, screening against Gram-negative bacterium *P. aeruginosa* showed that the activities of Cr(III) and Fe(III) complexes were less than that of HL. The Ni(II) complex showed no significant activity. The results against *E. coli* showed that the activities of Cr(III), Fe(III) and Ni(II) complexes were lower than that of HL.

The higher activity of metal complexes could be explained according to chelation theory. The polarity of the metal ion is reduced during chelation, due to the partial sharing of its positive charge with donor groups of the ligand and possible π-electron delocalization on the aromatic rings. This increases the lipophilic character, favouring permeation into the bacterial membrane, with blocking of the metal binding sites inside the enzymes of the microorganisms. This disturbs the respiration process of the cell and thus blocks the synthesis of proteins, which restricts further growth of the organisms.[38]

Also, there are other factors that also increase the activity, such as solubility, conductivity and bond length between metal and ligand. The mode of action may involve the formation of a hydrogen bond through the azomethine nitrogen and oxygen atoms with the active centres of the cell constituents, resulting in interference with the normal cell process.[39] The variation in the activity of different metal complexes against different microorganisms depends on the impermeability of the cell or differences in the ribosomes in the microbial cells. The lipid membrane surrounding the cell favours the passage of any lipid-soluble materials and it is known that liposolubility is an important factor controlling antimicrobial activity.[12,40]

TABLE 5 Anticancer activity of Schiff base ligand (HL) and complexes with 1,10-phen, using two cell lines (MCF-7 and HCT-116)

Compound	IC_{50} (μg)	
	MCF-7	HCT-116
Hl	>50	22.8
1,10-phen	35.6	21.3
$[Cr(L)(1,10\text{-phen})(H_2O)]Cl_2.2H_2O$	23.2	11.9
$[Mn(L)(1,10\text{-phen})(H_2O)]Cl.3H_2O$	23.4	28.3
$[Fe(L)(1,10\text{-phen})(H_2O)]Cl_2.2H_2O$	23.3	19.9
$[Co(L)(1,10\text{-phen})(H_2O)]Cl.2H_2O$	19.6	21.4
$[Ni(L)(1,10\text{-phen})(H_2O)]Cl.3H_2O$	16.3	23.5
$[Cu(L)(1,10\text{-phen})(H_2O)]Cl.2H_2O$	3.79	16.4
$[Zn(L)(1,10\text{-phen})(H_2O)]Cl.2H_2O$	42.1	10.8
$[Cd(L)(1,10\text{-phen})Cl].3H_2O$	16.5	24

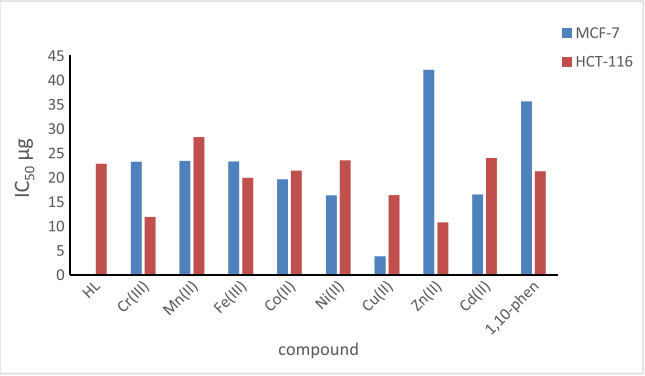

FIGURE 2 Anticancer activities of Schiff base ligand and its complexes with 1,10-phen

3.11.2 | Antifungal activity

The antifungal activities of HL, 1,10-phen and mixed ligand complexes against *A. fumigatus* and *C. albicans* are summarized in Table 4 and shown in Figure 1. The results for the activity against *A. fumigatus* confirmed that Cr(III), Co(II), Zn(II) and Cd(II) complexes had higher activity than that of HL. The Cr(III) complex had activity less than that of HL against *C. albicans*. The results also showed that the Ni(II) complex had no antifungal activity. The results may be due to the presence of chlorine ion in the complexes which may enhance antimicrobial activity due to the formation of hypochlorous acid which decomposes to HCl and O_2. The oxygen oxidizes the cellular components and destroyed the microbes. The results may also be explained by the combination of chlorine with membrane proteins and enzymes.[41,42]

In the present study, the low activity of the metal complexes may be due to their low lipophilicity, because of which penetration of the complexes through the lipid membrane is decreased. Hence, they can neither block nor inhibit the growth of the microorganisms.

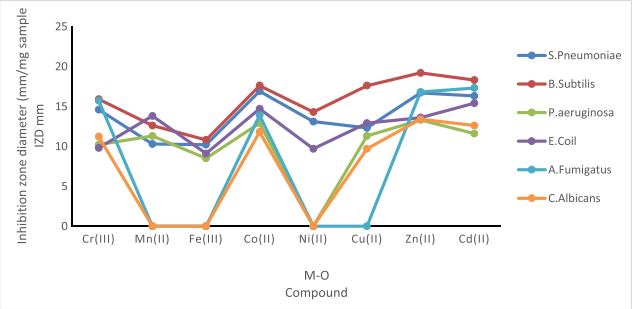

FIGURE 3 Relation between M—O bond strength and inhibition zone diameter of metal complexes

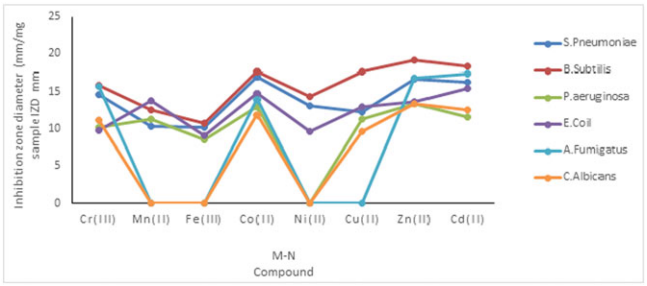

FIGURE 4 Relation between M—N bond strength and inhibition zone diameter of metal complexes

3.11.3 | Anticancer activity

The anticancer activities of HL, 1,10-phen and mixed ligand complexes using MCF-7 and HCT-116 cells in terms of IC_{50} (minimum concentration required to inhibit 50% of cell growth) are listed in Table 5 and shown in Figure 2. The results against breast cancer cell line showed that all metal complexes had IC_{50} higher than that of HL; however, the Cu(II) complex had the highest activity.[43] The complexes could be ordered according to their IC_{50} values as follows: Cu(II) > Cd(II) ≈ Ni(II) > Co(II) > Cr(III) ≈ Fe(III) ≈ Mn(II) > 1,10-phen > Zn(II). The results against colon cancer cell line showed that IC_{50} of Mn(II) and Cd(II) were higher than that of HL. The complexes may be ordered according to their IC_{50} values as follows: Zn(II) > Cr(III) > Cu(II) > Fe(III) > 1,10-phen > Co(II) > Ni(II) > Cd(II) > Mn(II).

1,10-Phen easily forms octahedral complexes with most transition metal cations. 1,10-Phen behaves as an anti-tumour agent because of its heteroaromatic planar and hydrophobic structure. In addition, this chelating agent shows better anti-tumour activity through chelation with metal ions. This will be more permeable through cell membranes eventually behave as carriers of anti-tumour agents.[44] The results of our study supported the finding that chelation of metal ions Cu(II), Cd(II), Ni(II), Co(II), Cr(III), Fe(III) and Mn(II) with HL and 1,10-phen enhanced the activity compared with 1,10-phen itself. This indicated an improvement of the anti-tumour potency upon coordination. The improvement of cytotoxic potency may be attributed to the positive charge of the metal increasing the acidity of coordinated ligand that bears protons, causing stronger hydrogen bonds which enhance the biological activity. It seems that changing the coordination sites and the nature of the metal ion has a clear effect on the biological activity by altering the binding ability of DNA. Abdel Rahman et al. reported that metal is suggested to smooth oxidative tissue injury through a free-radical-mediated trajectory analogous to the Fenton reaction[8] (Figure 3).

4 | CONCLUSIONS

A new Schiff base ligand and its mixed ligand complexes with 1,10-phen in a molar ratio of 1:1:1 were synthesized and characterized using elemental and spectroscopic analyses. The molar conductance values showed an electrolytic nature for all metal complexes except the Cd(II) complex. Electronic, magnetic and molecular formula data suggested an octahedral geometry for the metal complexes. The XRD patterns showed a crystalline nature for the metal complexes while an amorphous nature for HL. The free Schiff base and its mixed ligand complexes were screened against Gram-positive bacteria (*S. pneumoniae* and *B. subtilis*) and Gram-negative bacteria (*P. aeruginosa* and *E. coli*) and two fungal species (*A. fumigatus* and *C. albicans*). The data showed that most complexes had activity less than that of HL, and Mn(II), Fe(III) and Ni(II) complexes showed no significant antifungal activity. The metal complexes showed IC_{50} values higher than that of HL, and the Cu(II) complex showed the highest IC_{50} against breast cancer cell line (Figure 4).

REFERENCES

[1] L. Li, Q. Guo, J. Dong, T. Xu, J. Li, *J. Photochem. Photobiol. B* **2013**, *125*, 56.

[2] L. Shivakumar, K. Shivaprasad, H. D. Revanasiddappa, *Spectrochim. Acta A* **2012**, *97*, 659.

[3] B. H. M. Mruthy, D. B. Vivekanand, M. Raj, *Res. J. Pharm. Biol. Chem. Sci.* **2014**, *5*, 1057.

[4] S. Maddela, A. Makulaa, R. Maddela, *Toxicol. Environ. Chem.* **2014**, *96*, 1.

[5] A. Z. El-Sonbati, M. A. Diab, A. A. El-Bindary, M. I. Abou-Dobara, H. A. Seyam, *J. Mol. Liq.* **2016**, *218*, 434.

[6] G. S. Kumar, M. A. Ali, T. S. Choon, K. J. R. Prasad, *J. Chem. Sci.* **2016**, *128*, 391.

[7] W. Nkoana, D. Nyoni, P. Chellan, T. Stringer, D. Taylor, P. J. Smith, A. T. Hutton, G. S. Smith, *J. Organomet. Chem.* **2014**, *752*, 67.

[8] L. H. Abdel Rahman, A. M. Abu-Dief, R. M. El-Khatib, S. Abdel-Fatah, *J. Photochem. Photobiol. B* **2016**, *162*, 298.

[9] P. P. Sarmah, B. Deb, B. J. Borah, A. L. Fuller, A. M. Z. Slawin, J. D. Woollins, D. Kumar Dutta, *J. Organomet. Chem.* **2010**, *695*, 2603.

[10] H. F. Abd El-Halim, G. G. Mohamed, *J. Mol. Struct.* **2016**, *1104*, 91.

[11] S. K. Saha, A. Dutta, P. Ghosh, D. Sukulc, P. Banerjee, *Phys. Chem. Chem. Phys.* **2016**, *18*, 17898.

[12] W. H. Mahmoud, G. G. Mohamed, M. M. I. El-Dessouky, *Int. J. Electrochem. Sci.* **2014**, *9*, 1415.

[13] R. Neelaeni, S. Vasantha, R. Keerthana, S. Sivakolunthu, T. Angeline, *Asian J. Pharm. Clin. Res.* **2016**, *9*, 277.

[14] P. R. Reddy, S. Rajeshwar, B. Satyanarayana, *J. Photochem. Photobiol. B* **2016**, *160*, 217.

[15] Q. Wei, J. Dong, P. Zhao, M. Li, F. Cheng, J. Kong, L. Li, *J. Photochem. Photobiol. B* **2016**, *161*, 355.

[16] H. A. Flaschka, *EDTA Titration*, 2nd ed., Pergamon Press, New York **1964**, 81.

[17] A. I. Vogel, *Textbook of Quantitative Inorganic Analysis*, 4th ed., Longman, London **1978**.

[18] T. S. West, *Complexometry with EDTA and Related Reagents*, 3rd ed., DBH Ltd, Poole **1969**.

[19] A. C. Scott, in *Practical Medical Microbiology*, 13th ed. (Eds: J. G. Collee et al.), Churchill Livingstone, Edinburgh **1989**, 161.

[20] T. Mosmann, *J. Immunol. Methods* **1993**, *65*, 55.

[21] W. H. Mahmoud, N. F. Mahmoud, G. G. Mohamed, A. Z. El-Sonbati, A. A. El-Bindary, *J. Mol. Struct.* **2015**, *1095*, 15.

[22] H. F. Abd El-Halim, G. G. Mohamed, M. M. I. El-Dessouky, W. H. Mahmoud, *Spectrochim. Acta A* **2011**, *82*, 8.

[23] G. G. Mohamed, M. H. Soliman, *Spectrochim. Acta A* **2010**, *76*, 341.

[24] B. S. Creaven, M. Devereux, A. Foltyn, S. McClean, G. Rosair, V. R. Thangella, M. Walsh, *Polyhedron* **2010**, *29*, 813.

[25] I. Sheikhshoaie, S. Y. Ebrahimipour, N. Lotfi, J. T. Mague, M. Khaleghi, *Inorg. Chim. Acta* **2016**, *442*, 151.

[26] M. H. Soliman, A. M. M. Hindy, G. G. Mohamed, *J. Therm. Anal. Calorim.* **2014**, *115*, 987.

[27] D. Kivelson, R. Neiman, *J. Chem. Phys.* **1961**, *35*, 149.

[28] S. Chandra, X. Sangeetika, *Spectrochim. Acta A* **2004**, *60*, 147.

[29] B. J. Hathaway, D. E. Billing, *Coord. Chem. Rev.* **1970**, *5*, 143.

[30] A. Z. El-Sonbati, M. A. Diab, A. A. El-Bindary, G. G. Mohamed, S. M. Morgan, M. J. Abou-Dobara, S. E. Nozha, *J. Mol. Liq.* **2016**, *215*, 423.

[31] A. Z. El-Sonbati, M. A. Diab, A. A. El-Bindary, G. G. Mohamed, S. M. Morgan, *Inorg. Chim.* **2015**, *430*, 96.

[32] N. A. El-Ghamaz, A. Z. El-Sonbati, M. A. Diab, A. A. El-Bindary, G. G. Mohamed, S. M. Morgan, *Spectrochim. Acta A* **2015**, *147*, 200.

[33] S. Velumania, X. Mathew, P. J. Sebatain, S. K. Narayandass, D. Managlaraj, *Solar Energy Mater. Solar Cells* **2003**, *76*, 347.

[34] S. Sasavaraja, D. S. Salaji, M. D. Bedre, D. Raghunandan, P. M. P. Swamy, A. Venkatarmam, *Bull. Mater. Sci.* **2011**, *34*, 1313.

[35] M. M. Abo-Aly, A. M. Salem, M. A. Sayed, A. A. Abdel Aziz, *Spectrochim. Acta A* **2015**, *136*, 993.

[36] E. K. Efthimiadou, G. Psomas, Y. Sanakis, N. Katsaros, A. Karaliota, *J. Inorg. Biochem.* **2007**, *101*, 525.

[37] P. G. Lawrence, P. L. Harold, O. G. Francis, *Antibiot. Chemother.* **1980**, *5*, 1597.

[38] B. G. Tweedy, *Phytopathology* **1964**, *55*, 910.

[39] T. M. A. Ismail, A. M. Tawfik, S. M. Abu-El-Wafa, N. M. Ahmed, *Int. J. Pharm. Chem. Biol. Sci.* **2016**, *6*, 191.

[40] M. J. Pelczar, E. C. S. Chan, N. R. Krieg, *Microbiology: Concepts and Applications*, 6th ed., McGraw-Hill, New York **1999**, 478.

[41] L. M. Prescott, J. P. Harley, D. A. Klein, *Microbiology*, 2nd ed., W.C. Brown Communications, Dubuque, IA **1993**.

[42] S. S. Skandil, G. B. El-Hefnawy, E. A. Baker, *Thermochim. Acta* **2004**, *414*, 105.

[43] R. Křikavová, J. Vančo, Z. Trávníček, J. Hutyra, Z. Dvořák, *J. Inorg. Biochem.* **2016**, *163*, 8.

[44] M. Selvaganapathy, N. Raman, *J. Chem. Biol. Ther.* **2016**, *1*, 1.

How to cite this article: Abd El-Halim HF, Mohamed GG, Anwar MN. Antimicrobial and anticancer activities of Schiff base ligand and its transition metal mixed ligand complexes with heterocyclic base. *Appl Organometal Chem*. 2017; e3899. https://doi.org/10.1002/aoc.3899